Utilization of Flours from Hemp Stalks as Reinforcement in Polypropylene Matrix

İbrahim Kılıç,[a,*] Büşra Avcı,[b] İlkay Atar,[b] Nesrin Korkmaz,[c] Güngör Yılmaz,[d] and Fatih Mengeloğlu [b]

Utilization of hemp stalks (HS) was investigated as filler and maleic anhydride-grafted polypropylene (MAPP) as a coupling agent relative to some mechanical, physical, morphological, and thermal properties of polypropylene (PP) composites. The test sample manufacturing used 10, 15, 20, 25, 30, and 35 wt% of HS and 0 wt% or 3 wt% of MAPP. Test specimens were manufactured by combining extrusion and injection molding processes. Results showed that incorporating filler and MAPP increased the mechanical properties significantly. The utilization of HS filler or MAPP provided an improvement of 11.7% (samples containing 35 wt% HS and 3 wt% MAPP) improvement in tensile strength, 44.2% (samples containing 35 wt% HS and 3 wt% MAPP) in flexural strength, and 60.2% (samples containing 30 wt% HS and 0 wt% MAPP) in impact strength compared to neat PP. The scanning electron microscopy analysis provided visual evidence that MAPP improved adhesion between the filler and the polymer matrix. This study showed that using hemp stalks in composite manufacturing provided good overall properties.

DOI: 10.15376/biores.19.1.1494-1516

Keywords: Hemp stalk; Polypropylene; Natural fiber-based composites; Wood-plastic composites

*Contact information: a: Department of Material and Energy, Hemp Research Institute, Yozgat Bozok University, Yozgat, Turkey; b: Department of Forest Industry Engineering, Kahramanmaras Sutcu Imam University, Kahramanmaras, Turkey; c: Department of Basic Sciences and Health, Hemp Research Institute, Yozgat Bozok University, Yozgat, Turkey; d: Department of Field Crops, Yozgat Bozok University, Yozgat, Turkey; *Corresponding author: ibrahim.kilic@bozok.edu.tr*

INTRODUCTION

In recent years, increasing environmental awareness, concern about the depletion of oil resources, and concepts, such as sustainability and recycling, have encouraged the production of environmentally friendly materials. As a result of this new paradigm, interest in wood-plastic composites (WPCs) is also increasing. Wood-plastic composites are innovative materials in which wood or cellulosic fibers are mixed with various thermoplastics and additives and produced by extrusion, injection molding, and compression molding or thermoforming (pressing) methods (Klyosov 2007; Gardner *et al.* 2015; Kilic *et al.* 2023). Cellulosic fiber or wood refers to lignocellulosic fibers, such as flour, from various hardwood and softwood species (pine, poplar, beech, *etc.*), flour from timber particles, agricultural waste (wheat stalk, hemp stalk, *etc.*), bleached cellulose, and natural fibers (hemp, flax, kenaf, *etc.*) (Mohanty *et al.* 2002; Kim and Pal 2010; Mantia and Morreale 2011; Mengeloğlu and Çavuş 2020; Kilic *et al.* 2023). These fibers consist mainly of cellulose and lignin, and some of their properties, such as ease of processing, low density, low cost, and renewability, make them preferable (Mohanty *et al.* 2001;

Mengeloğlu and Karakuş 2012; Beaugrand *et al.* 2014). For this reason, WPCs are widely used in many industries (automotive, aerospace, electronics, construction, outdoor deck floors, railings, fences, landscaping timbers, park benches, *etc.*) because of their renewability, lightweight nature, and low-cost advantages (Kim and Pal 2010; Balla *et al.* 2019; Wu *et al.* 2020).

The matrices are an essential part of WPCs. The most common matrices used in WPCs are thermoplastic polymers, which are low in density and can be processed at low temperatures. The temperature at which lignocellulosic fibers degrade is an essential parameter in matrix selection. The thermal decomposition temperature of lignocellulosic fibers is generally regarded as being around 200 °C, and therefore, polymers that can be processed at temperatures lower than 200 °C are generally used in WPC production (Kim and Pal 2010; Summerscales *et al*. 2010; Pickering *et al*. 2016). Due to this limitation, thermoplastics that soften below this temperature, such as high-density polyethylene (HDPE), low-density polyethylene (LDPE), polyvinyl chloride (PVC), and polystyrene (PS), are used as the matrix (Klyosov 2007; Pickering *et al.* 2016).

Lignocellulosic fibers in thermoplastic polymers are used for two purposes. Firstly, the aim is to reduce the cost while providing a feature similar to neat polymer, and secondly, the aim is to increase performance properties compared to neat polymer (Kim and Pal 2010). Additionally, using lignocellulosic fibers in polymers has made them 'environmentally friendly or greener composites' (Netravali and Chabba 2003). There are many examples of using lignocellulosic fiber-reinforced polymer composites for these purposes (Summerscales *et al.* 2010; Pickering *et al.* 2016; Balla *et al.* 2019).

Lignocellulosic fibers are widely used in different industries as reinforcing agents in polymer composites, and some advantages and disadvantages of WPC are listed below (Mohanty *et al.* 2000, 2002; Gardner and Murdock 2010; Kim and Pal 2010; Faruk *et al.* 2012; Kılıç 2012; Koronis *et al.* 2013; Balla *et al*. 2019):

Advantages:

- WPCs are more environmentally friendly, renewable, and potentially recyclable.
- Using lignocellulosic fibers in plastic matrices makes them more rigid and can reduce overall cost;
- The lignocellulosic fibers use reduces the fossil-based raw materials amount and energy consumption;
- The production processes and disposal methods of WPCs are less harmful to the environment to neat plastics;
- The pressure properties of WPCs are superior to solid wood material;
- The maintenance cost of WPCs is lower than solid wood material;
- WPCs are resistant to biological effects compared to solid wood material;
- WPCs' dimensional stability and water absorption properties are better than solid wood.

Disadvantages:

- Moisture in the lignocellulosic-based areas inside WPCs may cause the formation of mold fungi;
- When lignocellulosic based fibers are added to thermoplastics, bleaching caused by sunlight may occur;
- WPCs are heavier and less rigid compared to solid wood material;
- Lignocellulosic fibers degrade over time at temperatures of 200 °C or higher. Therefore, polymer matrix selection in WPC production is limited.

The extrusion method is widely used in the WPC industry, and the composite products produced are generally used in areas such as deck floors, park and garden furniture, siding, *etc.* Another method used in the production of WPCs is the injection molding method, which is a processing technique used for the production of high-volume complex products. However, injection molding of high-filled WPCs is more troublesome than that of neat polymers due to the decreased fluidity of filled polymers. However, it is thought that producing WPCs with more complex shapes suitable for injection molding will become widespread in the coming years (Montanes *et al.* 2019). To reveal this potential, it is necessary to increase the studies and production in this field. This study is intended to contribute to the production of WPCs by injection molding. Considering the disadvantages of injection molding in producing WPCs, the proportion of lignocellulosic filler should be kept low in the injection method compared to the extrusion method. In previous studies, it was observed that lignocellulosic filler ratios ranged between 10% and 40% by weight (Lopez *et al.* 2012; Yan *et al.* 2013; Sullins *et al.* 2017; Maziero *et al.* 2019; Kilic *et al.* 2023; Vallejos *et al.* 2023). Considering these data, this study's hemp stalk filler level was limited to a maximum of 35%.

One of the most critical problems in WPCs production is poor bonding in the interaction of components due to poor wetting between the hydrophobic polymer matrix and hydrophilic fibers. The interface weakness between the polymer matrix and fibers can negatively affect many properties of WPCs. Because of the interfacial weakness, the zones of contact between the components fail to optimally transfer stress between the two phases when force is loaded, especially with respect to mechanical properties (Klyosov 2007). For this reason, coupling agents are used to improve compatibility and adhesion between fibers and polymers. Coupling agents are vital in improving the compatibility and adhesion between polar lignocellulosic fibers and non-polar polymeric matrices. Therefore, coupling agents utilization in WPC manufacturing is a standard method preferred for improving the mechanical properties of composites (Lu *et al.* 2000). Borysiak *et al.* (2011) reported that one of the most commonly used methods to improve adhesion between composite components is to use maleic anhydride grafted polypropylene (MAPP). In previous studies, it has been observed that coupling agents were used in the range of 2 to 10% in the production of WPCs and that the optimum properties were often found in the range of 3 to 5% (Çetin *et al.* 2000; Li *et al.* 2001; Panthapulakkal and Sain 2007; Oksman *et al.* 2009; Maziero *et al.* 2019; Díaz *et al.* 2020; Başboğa *et al.* 2022; Kilic *et al.* 2023; Vallejos *et al.* 2023). Considering the literature studies, in this study, MAPP was used at 0% and 3% by weight in the formulations of composites.

The components of industrial hemp that are mainly used in composites are its bast fibers (the outer part of the stalks) and hurd (the inside woody part of the stalks). Depending on the seed variety and planting conditions, hemp stalks comprise approximately 20 to 30% of bast fibers and 70 to 80% of hurds. Bast fibers are known as the most valuable part of the stalk and are high in cellulose and low in lignin. Hurds comprise the rest of the bast fibers and are higher in lignin (Borysiak *et al.* 2011; Shahzad 2011; Kurek 2013). Because the hurds and bast fibers have different properties, they have the potential for use in different areas. However, producing primary bast fibers is labor-intensive (Borysiak *et al.* 2011). For this reason, considering the difficulties and costs of obtaining these fibers separately, it becomes crucial to develop the usage areas of hemp stalks as a whole (hurd + bast) (Mengeloğlu 2020). In previous studies, generally, bast and hurd parts were evaluated separately as fillers in polymer matrices instead of utilizing hemp stalks as a whole (Beckermann and Pickering 2008; Khoathane *et al.* 2008; Kakroodi *et al.* 2012;

Lopez *et al.* 2012; Yan *et al.* 2013; Beaugrand *et al.* 2014; Rey *et al.* 2017; Sullins *et al.* 2017; Vilasecaa *et al.* 2018; Panaitescu *et al.* 2019; Berzin *et al.* 2020; Díaz *et al.* 2020; Rouway *et al.* 2020; Wu *et al.* 2020; Vilaseca *et al.* 2020;Burgada e*t al.* 2021; Han *et al.* 2021; Manaia and Manaia 2021; Wu *et al.* 2021). However, as far as the authors know, studies using whole hemp stalks together are limited. This study focused on evaluating hemp stalks as a whole (bast + hurd) as filler in wood-plastic composites (WPCs). For this purpose, flours obtained from hemp stalks were used as filler in WPCs production. The produced composites' mechanical, physical, thermal, and morphological properties were examined.

EXPERIMENTAL

Materials

Polypropylene (PP) (MH 418; density 0.905 g/cm^3, MFI 4.7 g/10 min, melting point 163 °C, Petkim Petrochemical Co., Türkiye) and hemp stalk (HS) were used as thermoplastic matrix and lignocellulosic filler, respectively. Insitu Green Technologies Industry and Trade Inc. Burdur, Türkiye, donated the hemp stalks (*Cannabis sativa* L.). Maleic anhydride-grafted polypropylene (MAPP) (Licocene® PP MA 7452 by Clariant, Berlin, Germany, melting point 155 to 161 °C, density 0.92 to 0.94 g/cm^3) was used as coupling agent.

Methods

The HS were granulated into different mesh-sized flour by Wiley Mill (Altundal, Kahramanmaraş, Türkiye) without being separated into bast fiber and hurd. The HS flours that passed through 10-mesh screen and stayed on an 80-mesh screen were dried and used before production. Since hemp stalks were used as a whole (bast + hurd) without being separated from the bast fibers, it was observed that there were lumps formed in the sieves due to the bast fibers during the sizing process. For this reason, hemp flours in the 10 to 80 mesh screen range were used. The drying process was continued at 103 ± 2 °C for 24 h until the moisture was reduced below 1%.

Composite Compounding

The WPCs were manufactured by combining extrusion and injection molding processes. The WPCs pellets were produced by the extrusion method, and then test specimens were produced from these pellets by the injection molding method (Fig. 1). The experimental design for composite manufacturing is given in Table 1. Depending on the formulation, the blends were compounded under heat. The blends were compounded in a laboratory-type single screw extruder at 50 rpm speed, at temperatures from feed zone to die of 180, 185, 190, 195, and 200 °C. The extruded compounds were cooled in a water pool (23 °C ± 2) and then granulated into pellets. The pellets were dried below 1% in an oven at 103 (± 2 °C) for 24 h before manufacturing WPC specimens by injection molding. The test specimens (Fig. 2) were produced with injection molding (HAIDAHDX–88, Ningbo, China). Injection molding conditions were as follows: injection temperature 170, 180, 185, 190, and 190 °C (from feed zone to die), injection speed 85 mm/s, injection pressure 9 to 10 MPa, and cooling time 40 s. Before testing, the specimens were conditioned in a climate cabinet at 23 (± 2) °C temperature and 65 (± 2%) relative humidity. Five specimens for each group were tested for the determination of properties of WPCs.

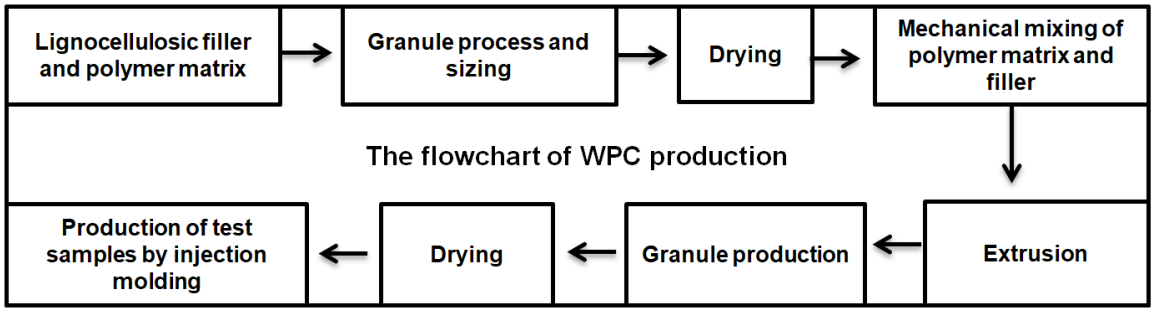

Fig. 1. Flowchart of WPC production

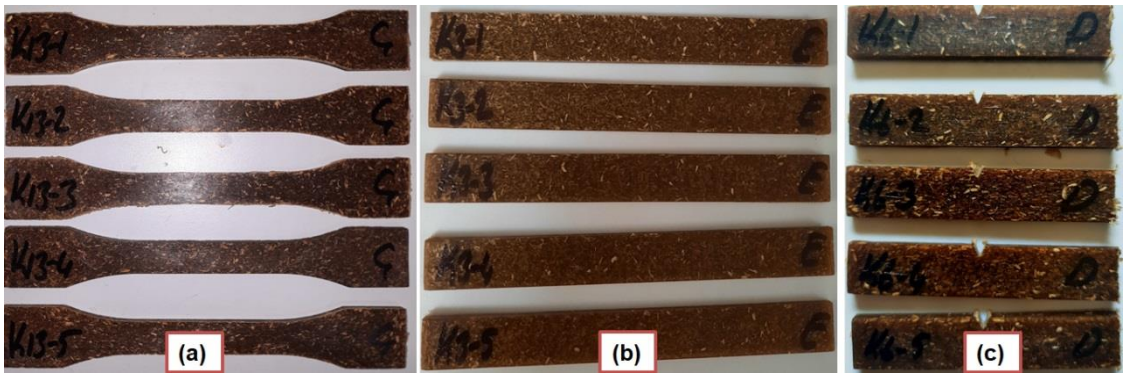

Fig. 2. Test specimens: (a): tensile specimens; (b): flexural specimens; (c): notched impact specimens

Table 1. Experimental Design for Composites Manufacturing

No.	ID	Polypropylene (PP) (%)	Hemp Stalk Flours (%)	Coupling Agent (MAPP) (%)
1	H_0M_0	100	0	0
2	H_0M_3	97	0	3
3	$H_{10}M_0$	90	10	0
4	$H_{10}M_3$	87	10	3
5	$H_{15}M_0$	85	15	0
6	$H_{15}M_3$	82	15	3
7	$H_{20}M_0$	80	20	0
8	$H_{20}M_3$	77	20	3
9	$H_{25}M_0$	75	25	0
10	$H_{25}M_3$	72	25	3
11	$H_{30}M_0$	70	30	0
12	$H_{30}M_3$	67	30	3
13	$H_{35}M_0$	65	35	0
14	$H_{35}M_3$	62	35	3

Determination the Properties of WPCs

Physical properties of WPC specimens, such as density and water absorption, and mechanical properties of WPC specimens, such as tensile strength (TS), tensile modulus (TM), elongation at break (EatB), flexural strength (FS), flexural modulus (FM), and impact strength (IS-notched), values were determined according to the relevant standards. In addition, morphological and thermal analyses of WPCs specimens were determined.

Density

Density was measured according to the ASTM D792-20 (2020) water displacement technique using test specimens in the size of 20 mm × 20 mm × 4 mm. Five experimental specimens were used for each group. The weights of the specimens were determined with 0.001 g accuracy. The density was calculated through Eq. 1,

$$D = d_s \, x \, \frac{a}{(a+w-b)} \, (g/cm^3) \quad (1)$$

where D is density (g/cm^3), a is apparent mass of specimen, without wire or sinker, in air (g), b is apparent mass of specimen completely immersed and of the wire partially immersed in liquid (g), w is apparent mass of totally immersed sinker and of partially immersed wire (g), and d_s is the density of water (0.9975 g/ cm^3 at 23 °C ± 0.10).

Water Absorption

Five specimens (20 mm × 20 mm × 4 mm) were submerged in water at room temperature (23 °C ± 1) for 2, 24, 48, 168, 336, 504, and 672 h. For each given measurement hour increment, specimens' weight was measured after wiping the water on the specimen's surface. The water absorption was calculated through Eq. 2,

$$WA\ (\%) = \frac{W_e - W_i}{W_i} \, x \, 100 \quad (2)$$

where WA is water absorption rate (%), W_i is initial weight of the specimen (g), and W_e is weight of the specimen after absorption of water (g).

Tensile Strength, Tensile Modulus and Elongation at Break

Tensile property tests were implemented using the Zwick 10 KN (Zwick/Roell, Ulm, Germany) instrument. Tensile strength, tensile modulus, and elongation at break of the produced composite specimens were determined according to the ASTM D638 (2010) standard. The dimensions (length x width x thickness) of the test specimens for tensile properties were 165 mm x 13 mm x 4mm (Dog Bone shape). The experiments were performed in 5 replicates, while the test speed was kept at 5 mm/min. Through averaging the data, the results of the tensile properties were determined. The tensile properties were calculated through tensile strengths (Eq. 3), tensile modulus (Eq. 4), and elongation at break (Eq. 5).

$$TS = \frac{P_{max}}{a*b} \quad (3)$$

In Eq. 3, TS is tensile strength (N/mm^2), P_{max} is maximum load (N), and $a*b$ is cross-sectional dimensions of the specimens (mm^2).

$$TM = \frac{\partial TS}{\varepsilon} \quad (4)$$

In Eq. 4, TM is tensile modulus (N/mm^2), ∂TS is tensile strength (N/ mm^2), and ε is unit elongation at break during tensile test.

$$\varepsilon = \frac{\Delta L}{L_0} x100 \quad (5)$$

In Eq. 5, ε is elongation at break (%), ΔL is unit elongation (mm), and L_0 is specimen size (mm).

Flexural Strength and Flexural Modulus

Flexural property tests were implemented using the Zwick 10 KN (Zwick/Roell, Ulm, Germany) instrument. Flexural strength and flexural modulus of the produced composite specimens were determined according to the ASTM D790 (2010) standard. The dimensions (length x width x thickness) of the test specimens for flexural properties were 165 mm x 13 mm x 4 mm. The experiments were conducted in 5 replicates while test speed was kept at 2 mm/min. The distance between the centers of the support span on which the specimens were placed was set to 80 mm. Through averaging the data, the results of the flexural properties were determined. The flexural properties were calculated through flexural strengths (Eq. 6), and flexural modulus (Eq. 7).

$$FS = \frac{3*P_{max}*L}{2*b*h^2} \quad (6)$$

In Eq. 6, FS is flexural strength (N/mm^2), P_{max} is maximum load applied at fracture (N), L is distance between the centers of support span (mm), b is width of the specimen (mm), and h is thickness of the specimen (mm). Flexural modulus was calculated as follows,

$$FM = \frac{\Delta F*L}{4*b*h^3*\Delta f} \quad (7)$$

where FM is flexural modulus (N/mm^2), ΔF is force equal to the difference between the arithmetic averages of the lower and upper limits of the loading in the elastic deformation region (N), L is distance between support span, Δf is deflection in the net flexural area is the difference between the arithmetic averages of the results of the deflections measured at the lower and upper limits of the loading (mm), b is width of the specimen (mm), and h is thickness of the specimen (mm).

Impact Strength (Notched)

An HIT5, 5P (Zwick) device was used for IS testing on notched specimens. The notches were added using a Polytest notching cutter by RayRan™. Impact strength of the produced composite specimens was determined according to the ASTM D256 (2010) standard. The dimensions (length x width x thickness) of the impact test specimens were 65 mm x 13 mm x 4 mm. Five specimens were used for each group and impact strength results were determined by averaging the data. The impact strength was calculated by Eq. 8,

$$IS = \frac{Q}{a*b} \quad (8)$$

where IS is the impact resistance (kJ/m²), Q is energy required to break the test specimen (kJ), and $a*b$ are the dimensions of the test specimen in radial and tangential directions, respectively (m²).

Scanning Electron Microscope

A scanning electron microscope (SEM), with the help of the Everhart–Thornley detector (ETD), model Zeiss Gemini 300 (Carl Zeiss, Oberkochen, Germany) was used to examine the morphology of the of the composites. First, the composite specimens were dipped into liquid nitrogen and then fractured surface was obtained for SEM characterization. Finally, the samples were coated with gold powders for 120 s at 10 mA using a Leica ACE600 device (Wetzlar, Germany) to provide electrical conductivity. The SEM images were taken at a magnification of 250X.

Thermogravimetric Analysis (TGA)

Thermogravimetric (TGA/DTGA) analysis of composite specimens was performed using an EXSTAR SII TG/DTA 6300 device (Labx, Midland, Canada). For analyses, the specimens were heated from 25 to 800 °C, using a nitrogen flow rate of 100 mL/min at a heating rate of 10 °C/min.

Statistical Analysis

Design-Expert®, version 13 (State-Ease, Inc., Minneapolis, MN, USA) software, was used for statistical analysis. Two-way analysis of variance (ANOVA) tests were performed to observe the effects of the filler amounts and coupling agent on the physical and mechanical properties of the composite specimens.

RESULTS AND DISCUSSION

In this study, some mechanical, physical (density and water absorption), morphological (SEM), and thermal (TGA, DSC) properties of PP-based composite specimens-filled hemp stalks and MAPP were determined.

Table 2. Mechanical Properties of Test Specimens

ID	TS (MPa)	TM (MPa)	EatB (%)	FS (MPa)	FM (MPa)	IS (kJ/m²)
H_0M_0	28.80* (0.24)**	650.24 (13.80)	-	40.18 (0.67)	1188.37 (22.02)	2.59 (0.30)
H_0M_3	28.75 (0.51)	639.19 (11.768)	-	39.95 (1.68)	1199.80 (56.81)	2.69 (0.28)
$H_{10}M_0$	26.49 (0.53)	734.41 (12.24)	7.53 (0.66)	44.11 (0.97)	1611.37 (76.58)	3.29 (0.18)
$H_{10}M_3$	28.09 (0.75)	743.15 (14.27)	7.33 (0.32)	46.43 (1.47)	1622.36 (86.55)	2.91 (0.15)
$H_{15}M_0$	26.39 (0.27)	841.78 (22.42)	6.25 (0.58)	46.25 (1.18)	1837.46 (57.98)	3.83 (0.33)
$H_{15}M_3$	28.86 (0.39)	865.08 (13.57)	5.53 (0.16)	50.57 (0.67)	1955.34 (70.85)	3.23 (0.24)
$H_{20}M_0$	25.72 (0.34)	897.83 (38.04)	5.63 (0.24)	47.44 (0.55)	2058.17 (44.20)	4.05 (0.30)
$H_{20}M_3$	29.46 (0.68)	966.69 (30.92)	4.80 (0.50)	53.92 (0.38)	2224.17 (49.02)	3.66 (0.11)
$H_{25}M_0$	25.22 (0.80)	1034.81 (22.22)	4.19 (0.10)	49.68 (2.21)	2386.26 (42.89)	3.97 (0.37)
$H_{25}M_3$	30.38 (0.64)	1106.24 (31.51)	4.15 (0.15)	57.04 (1.55)	2610.98 (77.03)	3.79 (0.21)
$H_{30}M_0$	24.76 (0.60)	1087.52 (22.75)	3.77 (0.27)	47.78 (0.51)	2539.88 (114.90)	4.15 (0.13)
$H_{30}M_3$	31.70 (0.45)	1213.33 (28.56)	3.68 (0.23)	57.28 (1.55)	2780.82 (122.24)	3.78 (0.34)
$H_{35}M_0$	23.78 (0.53)	1098.62 (16.59)	3.58 (0.14)	47.04 (1.24)	2691.40 (93.17)	3.97 (0.15)
$H_{35}M_3$	32.16 (1.03)	1316.90 (11.18)	3.38 (0.11)	57.96 (0.39)	3070.31 (99.06)	3.77 (0.15)

Five specimens for each group were tested, *: Average values, **: standard deviation

Mechanical Properties of WPCs

Tensile strength (TS), tensile modulus (TM), elongation at break (EatB), flexural strength (FS), flexural modulus (FM), and impact strength (IS) properties were the mechanical properties studied. The results obtained from the mechanical properties of the test specimens are shown in Table 2.

The TS, TM, and EatB interaction graphs are presented in Figs. 3a, 3b, and 3c, respectively. In all three figures, the groups without MAPP are shown with red lines, and groups with MAPP are shown with green lines.

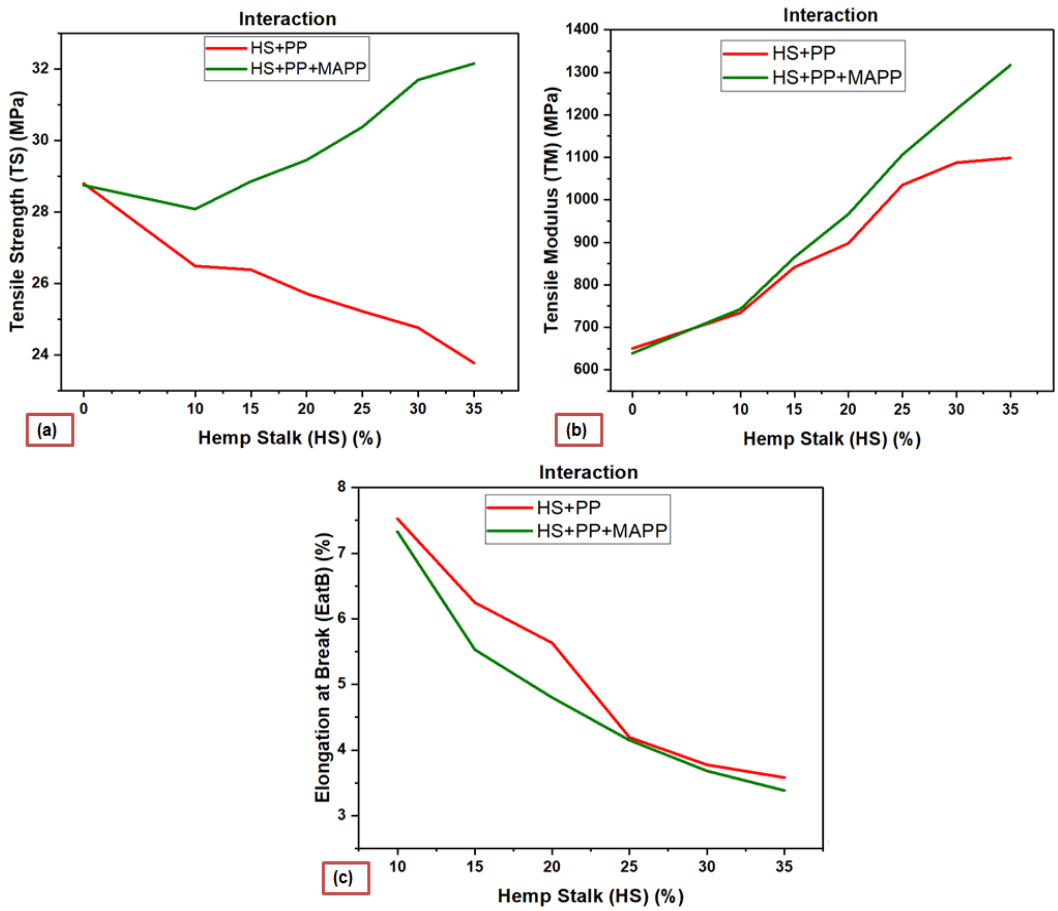

Fig. 3. Interaction graphs of HS and MAPP loading on composites: (a): tensile strength; (b): tensile modulus; (c): elongations at break

The TS values of the test specimens were in the range of 23.8 to 32.2 MPa. The lowest and the highest TS values were observed in $H_{35}M_0$ and $H_{35}M_3$ coded specimens, respectively. Statistical analysis showed that HS loading level and MAPP significantly affected the TS values ($P < 0.0001$). The differential of the TS of composites compared with those of neat PP was closely related to the composition of filler, matrix, and coupling agent. The TS values were reduced with increasing concentration of HS in the polypropylene matrix. It is thought that as the increased concentration of HS in the polypropylene matrix increases the interfacial area, the weakening of interfacial bonding between hydrophilic filler and hydrophobic polymer matrix decreases the TS (Yang *et al.* 2004; Maziero *et al.* 2019; Eroğlu *et al.* 2023; Kilic *et al.* 2023). Similar strength reduction by lignocellulosic filler addition due to the worsening interfacial bond between

the polymer matrix and the filler was also reported by others (Bledzki and Faruk 2003; Yang *et al*. 2007; Narlıoğlu *et al.* 2018; Çavuş 2020; Çavuş and Mengeloğlu 2020; Başboğa *et al.* 2022; Kilic *et al.* 2023). The MAPP, which was utilized as a coupling agent in the formulation to improve the adhesion between filler and polymer matrix, dramatically increasing the composites' TS values. Compared to the TS of composites without MAPP, an average improvement of approximately 18.5% was observed with the addition of MAPP. This was attributed to the fact that MAPP creates an efficient stress transfer by increasing the adhesion strength between the filler and polymer matrix surfaces (Langhorst *et al*. 2018; Çavuş and Mengeloğlu 2020; Kilic *et al.* 2023). However, in the specimens produced with MAPP, the specimens with 15% filler ratio had tensile strength values similar to pure PP, while the specimens with 10% filler ratio provided lower tensile strength values. It is thought that this is due to the inability to provide efficient transfer from the polymer to the fibers due to the low filling ratio.

Statistical analysis showed that the HS loading level and presence of MAPP significantly affected TM values ($P < 0.0001$). The TM values of the test specimens ranged from 650 to 1317 MPa. The lowest and highest TM values were observed in the unfilled PP and $H_{35}M_3$ (35% HS filler and 3% MAPP), respectively. It is clear from Fig. 1b that the tensile modulus values of the composites increased with increasing HS filler content. The TM values of test specimens increased independently of MAPP. Lignocellulosic fibers have higher modulus compared to polymer matrix (Çavdar *et al*. 2011). As a result, the addition of a high-modulus lignocellulosic fiber into the polymer matrix increased the resulting composite modulus values due to the rule of mixture (Mengeloğlu and Karakuş 2012; Çavuş and Mengeloğlu 2020; Kilic *et al.* 2023). The presence of MAPP in the formulation increased the modulus values of composites nearly 9% due to the increased adhesion between the polymer matrix and the filler.

Manufactured test specimens had EatB values of 3.38 to 7.53%. The testing machine measured elongation up to 400%. Statistical analysis was not conducted because HS unfilled samples (H_0M_0, H_0M_3) were not broken within this elongation limit. These groups are not shown in Fig. 1c. Statistical analysis showed that both the HS rates ($P < 0.0001$) and MAPP ($P = 0.0002$) had a significant effect on EatB values. The EatB values decreased significantly with increasing HS loading levels in composite samples, a common observation in WPCs. As the percentage of lignocellulosic filler loading in WPCs increased, the composite's brittleness increased and turned into a more rigid structure. In addition, EatB values in samples containing MAPP decreased slightly compared to samples without MAPP. This is because the samples with MAPP became more brittle due to the improved interfacial adhesion between the filler and the polymer matrix. Consequently, the elongation at break (EatB) values of WPCs decreased. Similar results were reported in previous studies (Zaini *et al.* 1996; Balla *et al.* 2019; Çavuş and Mengeloğlu 2020; Başboğa *et al.* 2023; Kilic *et al.* 2023).

The test specimens' FS and FM interaction graphs are presented in Fig. 4a and 4b, respectively. The groups without MAPP are shown with red lines in the two figures, and groups with MAPP are shown with green lines. The FS values of the test specimens ranged from 40.0 to 58.0 MPa. Statistical analysis showed that both the percentage of HS loading and MAPP significantly affected FS values ($P < 0.0001$). Despite MAPP, the FS values enhanced considerably with an increasing percentage of HS loading in the PP matrix. Compared to the FS values of unfilled and HS-filled PP, an average improvement of 17% was observed in the groups without MAPP and an average improvement of 34% in the groups with MAPP. It is thought that after a lignocellulosic fiber with higher bending

strength is compounded into the polymer matrix, effective load transfer from the polymer to the fiber occurs when force is applied (Başboğa 2023). Furthermore, MAPP addition to HS-filled formulations resulted in an average improvement of approximately 14.5% in FS values. This is attributed to the improved adhesion strength between filler and polymer matrix. It has been reported that effective stress transfer from the PP matrix to lignocellulosic fibers occurs when there is significant binding of MAPP in WPCs (Langhorst *et al.* 2018; Kilic *et al.* 2023). Manaia and Manaia (2021) reported that the improved interfacial adhesion between the polymer matrix and hemp fiber largely determines the flexural strength of composites, as the load in flexural tests is transferred through the matrix-fiber interface. Other studies reported similar results using different lignocellulosic fillers (Bledzki and Faruk 2003; Kim *et al.* 2007; Çavuş and Mengeloğlu 2020; Kilic *et al.* 2023).

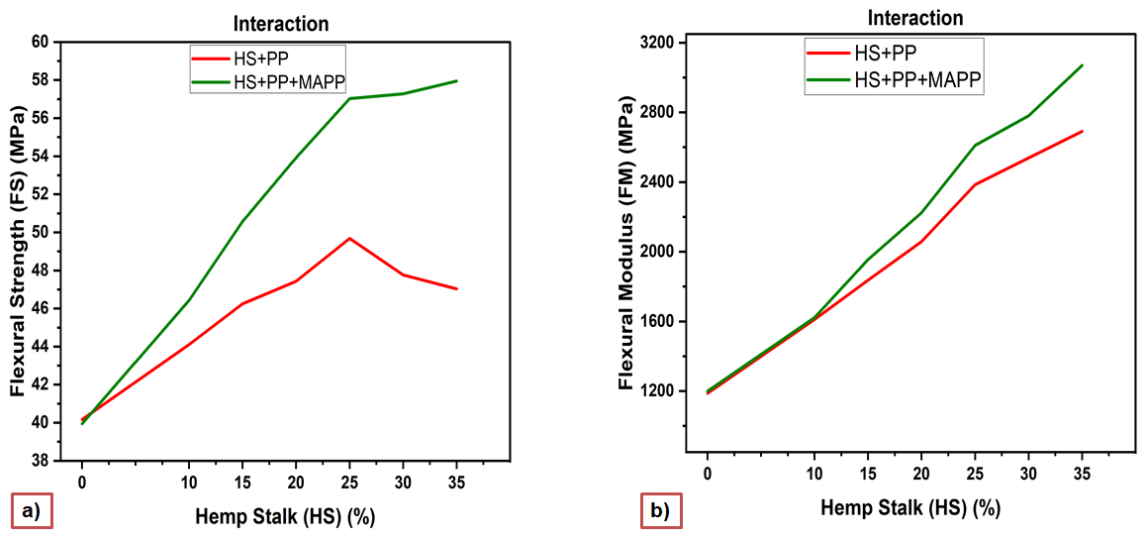

Fig. 4. Interaction graphs of HS and MAPP loading on composites: (a): flexural strength; (b): flexural modulus

The FM values of the manufactured specimens ranged from 1188 to 3070 MPa. Statistical analysis demonstrated that HS loading level and MAPP significantly affected FM ($P < 0.0001$). Independent of MAPP, FM values increased substantially with increasing HS filler compared to unfilled PP. Lignocellulosic fibers are a higher modulus material than polymers, and higher fiber concentration demands higher stress for the same deformation (Karmarkar *et al.* 2007; Kilic *et al.* 2023). Furthermore, adding MAPP to the formulations slightly increased the FM values by the improved interfacial adhesion between the hemp fiber and the polymer matrix, enabling increased stress transfer from the matrix to the filler. As a result, lignocellulosic fiber-reinforced polymer composites can achieve a higher flexural modulus than unfilled polymers. Similar results have been reported in other studies (Espinach *et al.* 2013; Mengeloğlu and Çavuş 2020; Başboğa 2023).

The interaction graphs of the notched IS are presented in Fig. 5. The IS values of the manufactured composite specimens ranged from 2.59 to 4.15 kJ/m^2. The groups without MAPP are shown with a red line, and groups with MAPP are shown with a green line. Statistical analysis showed that the HS filler loading level and MAPP significantly affected IS values ($P < 0.0001$). The IS values enhanced within a creased percentage of HS

loading to the polymer matrix. An approximate 60% increase in IS values was observed in 30% of HS filled-PP composite samples compared to unfilled-PP. Impact strength is related to the toughness of the composite and is a measure of the ability of the composite to resist breakage under load applied (Panthapulakkal and Sain 2007). Yuan *et al.* (2008) reported that more energy is needed to break the fillers when breaking fiber-filled polymers than unfilled polymers. Burgada *et al.* (2021) reported that the ability to absorb and dissipate energy in the polymer matrix could be attributed to fiber fillers. Panthapulakkal and Sain (2007) also reported similar results and attributed the ability of fibers acting as stress-transferring to play an essential role in the impact strength of WPCs. Although the IS values increased with the HS filler, lower IS values were obtained in specimens with MAPP than in specimens without MAPP. It is thought that with the addition of MAPP in WPCs, the composite's brittleness increases and the IS values decrease slightly. Other studies have also reported that coupling agents reduce IS values in WPCs (Mengeloğlu and Karakuş 2008; Langhorst *et al.* 2018; Kilic *et al.* 2023).

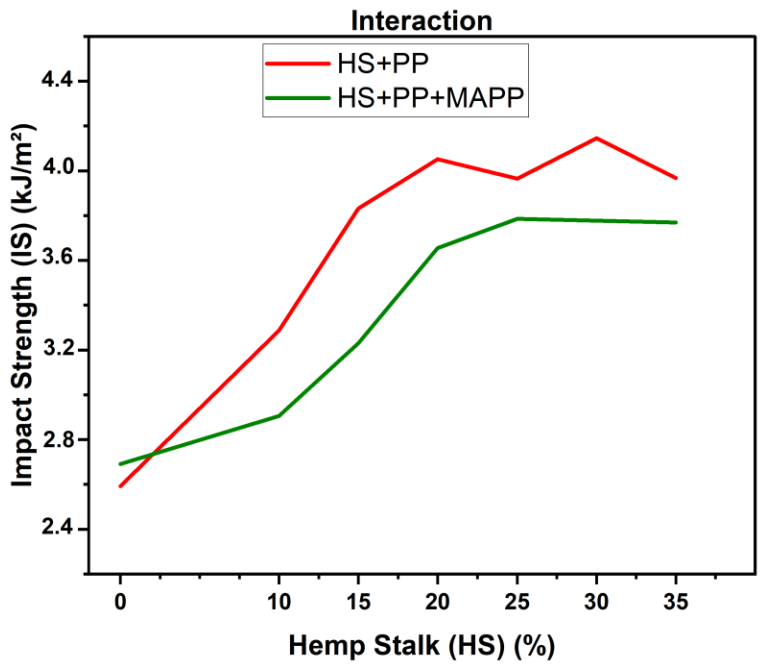

Fig. 5. Interaction graph of HS and MAPP loading on composites notched impact strength

Physical Properties of WPCs

Density values and water absorption rates were the physical properties studied. The density values and water absorption percentage are presented in Tables 3 and 4, respectively.

The density values obtained from the test specimens ranged from 0.879 to 0.984 g/cm^3. The lowest and the highest density values were observed in H_0M_0 and $H_{35}M_3$ coded specimens, respectively. The interaction graph of the HS fillers and MAPP on the density of composite specimens is presented in Fig. 6. Statistical analysis showed that filler loading level ($P < 0.0001$) and MAPP ($P = 0.0150$) had a significant effect on density. Higher density values were obtained in composite specimens as the percentage of HS filler loading increased. This increase is thought to be due to the higher cell wall density of lignocellulosic fibers (approximately 1.5 g/cm^3) than polymer (Stokke and Gardner 2003; Mengeloğlu and Karakuş 2008; Islam *et al.* 2013; Mengeloğlu *et al.* 2015; Kilic *et*

al. 2023). Clemons and Caufield (2005) reported high-pressure processes, such as injection molding, cause the lignocellulose's hollow fibers to collapse or to become filled with low molecular weight plastics.

Table 3. Average Density Values of Test Specimens

ID	Density (g/cm³)
H_0M_0	0.890* (0.002)**
H_0M_3	0.879 (0.012)
$H_{10}M_0$	0.906 (0.010)
$H_{10}M_3$	0.892 (0.010)
$H_{15}M_0$	0.913 (0.007)
$H_{15}M_3$	0.919 (0.009)
$H_{20}M_0$	0.921 (0.008)
$H_{20}M_3$	0.929 (0.006)
$H_{25}M_0$	0.939 (0.004)
$H_{25}M_3$	0.934 (0.011)
$H_{30}M_0$	0.950 (0.004)
$H_{30}M_3$	0.966 (0.009)
$H_{35}M_0$	0.947 (0.021)
$H_{35}M_3$	0.984 (0.003)

Five specimens for each group were tested, *: Average values, **: standard deviation

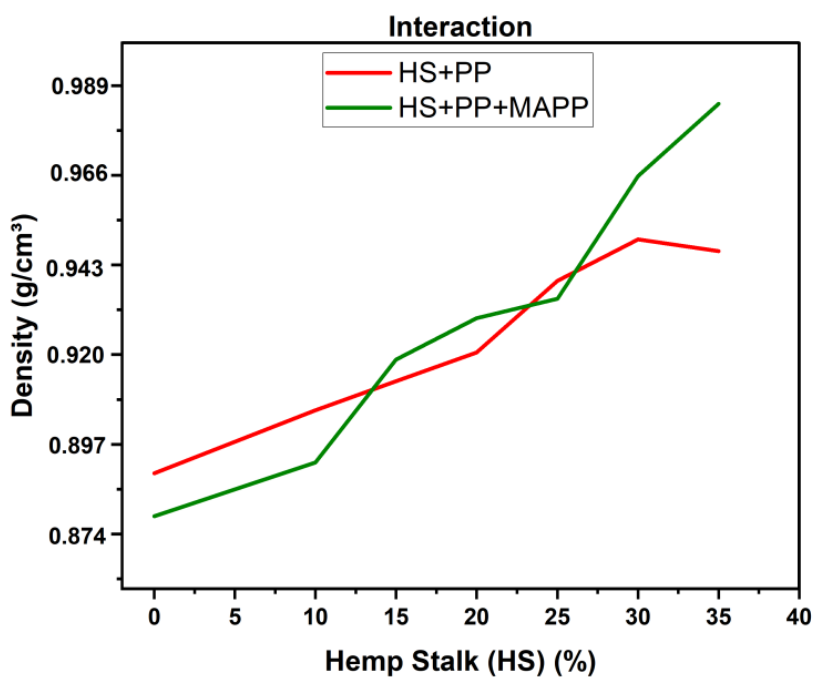

Fig. 6. Interaction graph of FFWS and MAPP loading on composites' density values

Table 4. Water Absorption Percentages of Test Specimens

ID	2 h	24 h	48 h	72 h	168 h	336 h	504 h	672 h
$H_{10}M_0$	0.08	0.15	0.22	0.21	0.22	0.45	0.81	0.81
$H_{10}M_3$	0.02	0.09	0.13	0.14	0.19	0.36	0.77	0.79
$H_{15}M_0$	0.18	0.23	0.32	0.60	0.71	0.81	0.99	1.01
$H_{15}M_3$	0.14	0.14	0.23	0.28	0.32	0.46	0.69	0.73
$H_{20}M_0$	0.14	0.32	0.41	0.41	0.64	0.66	1.14	1.17
$H_{20}M_3$	0.13	0.22	0.27	0.27	0.49	0.58	0.91	0.94
$H_{25}M_0$	0.31	0.31	0.33	0.35	0.35	0.80	1.06	1.06
$H_{25}M_3$	0.17	0.24	0.29	0.31	0.33	0.39	0.56	0.65
$H_{30}M_0$	0.38	0.51	0.76	0.72	1.31	1.86	2.33	2.66
$H_{30}M_3$	0.13	0.25	0.38	0.36	0.72	0.80	1.23	1.26
$H_{35}M_0$	0.38	0.71	1.00	1.08	1.29	2.59	3.30	3.71
$H_{35}M_3$	0.12	0.33	0.42	0.46	0.92	1.08	1.46	1.54

Note: Values are percentage change by weight (wt%)

The HS-filled PP composites' water absorption percentages after 2 h, 24 h, 48 h, 72 h, 168 h, 336 h, 504 h, and 672 h are given in Fig. 7. Because the data relating to PP water absorption is considered zero, water absorption data of unfilled PP are not included. In the columns in Fig. 7, the shaded columns show groups with MAPP, and the empty columns show groups without MAPP.

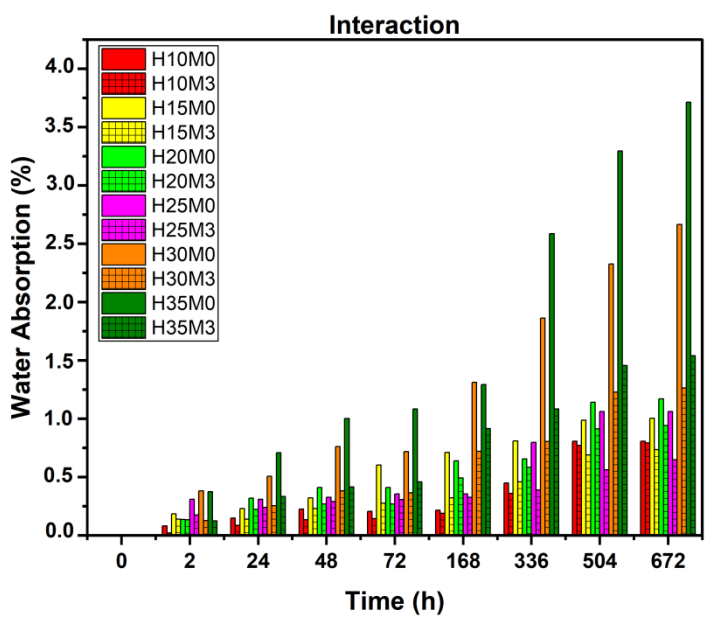

Fig. 7. The water absorption of the HS reinforced PP composites during 28 days of water immersion

The water absorption of test specimens ranged from the lowest (0.08%) to the highest (3.71%). Increasing filler content in composite specimens resulted in higher water absorption. The highest water absorption was obtained from the specimens consisting of 35%; the time the specimens stayed in water increased the water absorption. A more significant increase was observed in the water absorption, especially of the highly filled specimens (30% and 35%) after 72 h. The water absorption of WPCs is mainly affected by the structure of lignocellulosic fiber, and they may absorb more water than neat

thermoplastics. Lignocellulosic fibers have hydroxyl groups that interact with water molecules by hydrogen bonding. Thus, the results are sensitive to water (Çavdar *et al.* 2011). Lopez *et al.* (2012) attributed that to forming of an incompatible mixture of the two components and incorporating hydrophilic fibers inside a hydrophobic polymer matrix. Çavdar *et al.* (2023) reported that the incompatibility of the filler with the polymer matrix causes voids and increases the water absorption of the WPCs. However, if the lignocellulosic fiber is properly encapsulated during processing, the WPCs will absorb less water (Stokke and Gardner 2003). This has been observed in composites containing MAPP. Because the inclusion of MAPP in the formulations increased the compatibility between the fiber and the polymer matrix, the water absorption percentages of the composites were slightly improved. The improved adhesion between filler and polymer matrix in groups with MAPP is presented in SEM images.

Morphological Properties of WPCs

The morphology of the test specimens is presented in Fig. 8. Parts (a), (b), (c), and (d) of the figure show SEM images of the $H_{20}M_0$, $H_{20}M_3$, $H_{35}M_0$, and $H_{35}M_3$, respectively. In composites, samples without MAPP (Fig. 8a and 8c) show pullout, debonding, or gaps throughout the interphase between fibers and matrix. These gaps manifest the weak adhesion between fiber and polymer matrix. However, in composites with MAPP (Fig. 8b and 8d), a significant improvement in fiber/matrix adhesion and a compact interphase with fewer voids were observed. Fig. 8b shows a fiber entirely covered by the matrix, indicating the presence of improved adhesion between the filler and the polymer matrix. This result was also consistent with the improved mechanical properties (*e.g.*, tensile and flexural strength) of composites with MAPP. Previous studies also reported that the use of compatibilizers in WPCs improves the performance properties of composites (Kakroodi *et al.* 2012; Panaitescu *et al.* 2019; Çavus 2020; Çavus and Mengeloğlu 2020; Díaz *et al.* 2020; Kilic *et al.* 2023).

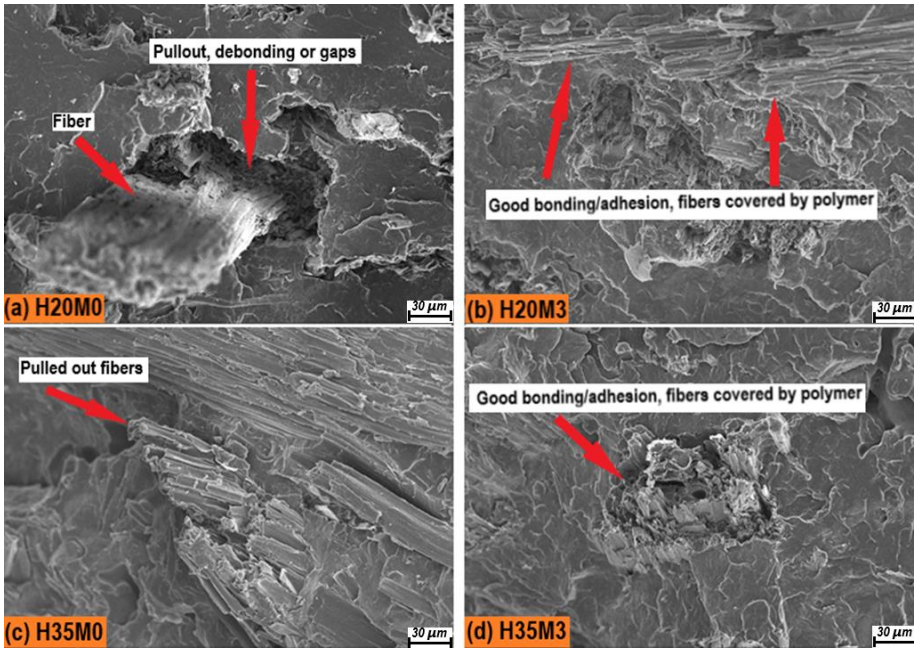

Fig. 8. SEM images of the sections broken under impact for composites: (a): $H_{20}M_0$; (b): $H_{20}M_3$; (c): $H_{35}M_0$; and (e): $H_{35}M_3$

Thermal Properties of WPCs

The composite specimens' TGA and DTGA (derivative thermogravimetric analysis) curves are presented in Figs. 9a and 9b, respectively. Fig. 9a shows the weight loss *versus* temperature curves, while Fig. 9b illustrates the corresponding first derivative curves. The TGA analyses were performed for H_0M_0, $H_{20}M_0$, $H_{20}M_3$, $H_{35}M_0$, and $H_{35}M_3$. In addition, the degradation onset temperature (T_{onset}), the temperature of degradation endset (T_{endset}), and degradation percentages at different stages of degradation of the composite specimens are presented in Table 5. A single-stage thermal degradation was observed in the specimens in TGA analysis. Considering the values in Table 5, the decomposition for the unfilled-PP started at approximately 216 °C and ended at around 479 °C. At the end of the second stage, the unfilled-PP exhibited 99.5% degradation. At the end of the test at 700 °C, neat polypropylene reached maximum degradation, and residue content reached 3%. A similar result was reported: unfilled PP was degraded entirely (Silveira *et al.* 2023). Additionally, at the end of the test at 700 °C, the $H_{20}M_0$, $H_{20}M_3$, $H_{35}M_0$, and $H_{35}M_3$ residue contents were 1.6, 1.6, 0.6, and 0.8%, respectively. Consequently, using MAPP in HS-filled composites showed no change in residue amounts.

Table 5. Thermal Parameters Obtained by TGA of Composites

ID	T_{onset} (°C)	T_{endset} (°C)	Mass Loss		
			At T_{onset} (%)	At T_{onset} - T_{endset} (%)	At 700 °C (%)
H_0M_0	216.2	479.1	0.5	99.5	0
$H_{20}M_0$	215.8	503.0	1.2	97.2	1.6
$H_{20}M_3$	251.2	481.9	1.5	96.9	1.6
$H_{35}M_3$	235.7	494.4	2.4	97.0	0.6
$H_{35}M_3$	238.2	503.8	2.4	96.7	0.8

When Figs.9a, 9b, and Table 5 were examined, it was observed that the thermal degradation of the composite specimens occurred in two different stages.

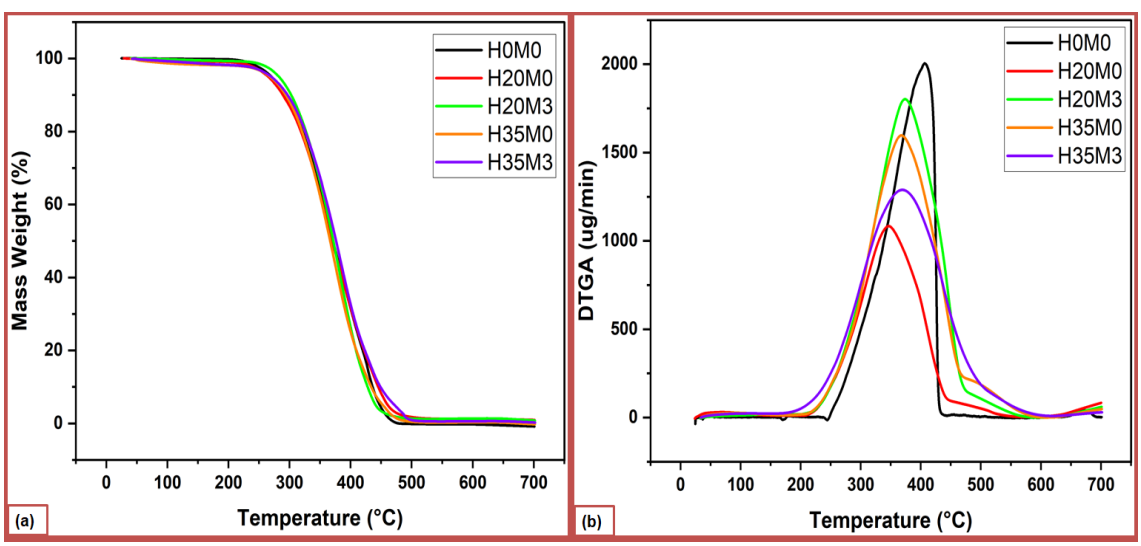

Fig. 9. Comparative TGA graphs of composites: (a): TGA curves; (b): DTGA curves

The first stage, which started at room temperature and was completed at T_{onset}, is generally associated with moisture loss in the composites. A similar result was reported by Silveira *et al.* (2023). With the increase of the HS filler ratio, the degradation rate in T_{onset}

increased, resulting in a 2.4% loss in 35% HS filled-PP. It is thought that this is because HS-filled composites contain more moisture. The second stage of the degradation started when the temperature reached approximately 215 °C, and above this temperature (T_{onset}-T_{endset} range), a rapid increase in the decomposition curve was observed.

While the T_{onset} temperature of unfilled-PP was approximately 216 °C, the T_{onset} temperatures of HS-filled-PP ranged between 216 and 251 °C. This difference is thought to be due to cellulose, hemicellulose, and lignin, the main components of hemp stalks. Others have also reported that these three components increase the thermal decomposition temperature in WPCs (Şeker Hirçin *et al*. 2021; Başboğa 2023). The second stage of the degradation started when the temperature reached approximately 215 °C, and above this temperature (T_{onset}-T_{endset} range), a rapid increase (Fig. 7a) in the decomposition curve was observed. The second degradation stage (T_{endset}) temperature in composite specimens ranged from 479 to 503 °C. With the addition of hemp stalk, the T_{endset} temperature value increased approximately 20 °C compared to the unfilled-PP.

CONCLUSIONS

This study evaluated the effect of hemp stalk flours and maleic anhydride-grafted polypropylene (MAPP) participation percentage on the mechanical, physical, morphological, and thermal properties of hemp stalk (HS) reinforced polypropylene (PP)-based composites. In the production of composites, 0, 5, 10, 15, 20, 25, 30, and 35% hemp stalk (HS) was loaded into the polypropylene matrix as filler, respectively, and 0 or 3% MAPP was used as a coupling agent. HS-filled polypropylene composites were successfully produced, and the following conclusions were reached:

1. Adding HS filler to the PP matrix increased the mechanical properties of the produced composites compared to neat PP.
2. Increasing the amount of HS filler increased the flexural strength, flexural modulus, tensile modulus, impact resistance, and density values of PP.
3. The tensile strength decreased with increasing HS amount, but the addition of MAPP caused a dramatic increase in tensile strength.
4. The flexural strength, flexural modulus, tensile strength, tensile modulus, and density values of composites with MAPP were higher than those without MAPP.
5. When the tensile strength (TS) and flexural strength (FS) of composites containing MAPP were compared to composites without MAPP, an average improvement of about 18.5% and 14.5%, respectively, was observed.
6. Increasing the amount of HS filler increased the water absorption percentages, but the inclusion of MAPP in the formulations slightly improved the water absorption rates of the composites.
7. Thermogravimetric analyses (TGA) were performed on groups selected among the produced composites. Weight losses in the first stage were observed as 0.5%, 1.2%, 1.5%, 2.4%, and 2.4% in the groups coded H_0M_0, $H_{20}M_0$, $H_{20}M_3$, $H_{35}M_0$, and $H_{35}M_3$, respectively. The amount of residue at 700 °C was observed as 0%, 1.6%, 1.6%, 0.6%, and 0.8% in the groups coded H_0M_0, $H_{20}M_0$, $H_{20}M_3$, $H_{35}M_0$, and $H_{35}M_3$, respectively.

8. The scanning electron microscopy (SEM) analysis showed that MAPP improved adhesion between the HS filler and the polypropylene matrix.

ACKNOWLEDGMENTS

This study was supported by The Scientific and Technological Research Council of Türkiye (TUBITAK—project Number 122O317).

We thank "Insitu Green Technologies Industry and Trade Inc." for providing hemp stalks.

REFERENCES CITED

ASTM D256 (2010). "Standard test for determining the Izod pendulum impact resistance of plastics," ASTM International, West Conshohocken, PA, USA.

ASTM D638 (2010). "Standard test for tensile properties of plastics," ASTM International, West Conshohocken, PA, USA.

ASTM D790 (2010). "Standard test methods for flexural properties of unreinforced and reinforced plastics and electrical insulating materials," ASTM International, West Conshohocken, PA, USA.

ASTM D792-20 (2020). "Standard test methods for density and specific gravity (relative density) of plastics by displacement," ASTM International, West Conshohocken, PA, USA.

Balla, V. K., Kate, K. H., Satyavolu, J., Singh, P., and Tadimeti, J. G. D. (2019). "Additive manufacturing of natural fiber reinforced polymer composites: Processing and prospects," *Composites Part B: Engineering* 174, article ID 106956. DOI: 10.1016/j.compositesb.2019.106956

Başboğa, İ. H., Kılıç, İ., Atar, İ., and Mengeloğlu, F. (2022). "Tropik ağaç türü olan dahoma (*Piptadeniastrum africanum*) odununun odun plastik kompozit üretiminde kullanımı [The usage of wood of dahoma (*Piptadeniastrum Africanum*), a tropic tree, in the production of wood plastic composite]," *Ormancılık Araştırma Dergisi [Forestry Research Journal]* 9 (Özel Sayı [Special Issue]), 271-280. DOI: 10.17568/ogmoad.1091247

Başboğa, H. I. (2023). "Polypropylene-based composites reinforced with waste tropic wood flours: Determination of accelerated weathering resistance, tribological, and thermal properties," *BioResources* 18(4), 7251-7294. DOI: 10.15376/biores.18.4.7251-7294

Beaugranda, J., Nottez, M., Konnerth, J., and Bourmaud, A. (2014). "Multi-scale analysis of the structure and mechanical performance of woody hemp core and the dependence on the sampling location," *Industrial Crops and Products* 60, 193-204. DOI: 10.1016/j.indcrop.2014.06.019

Beckermann, G. W., and Pickering, K. L. (2008). "Engineering and evaluation of hemp fibre reinforced polypropylene composites: Fibre treatment and matrix modification," *Composites: Part A: Applied Science and Manufacturing* 39(6), 979-988. DOI: 10.1016/j.compositesa.2008.03.010

Berzin, F., Lemkhanter, L., Marcuello, C., Chabbert, B., Béghin, V. A., Molinari, M., Castellani, R., and Vergnes, B. (2020). "Influence of the polarity of the matrix on the

breakage mechanisms of lignocellulosic fibers during twin-screw extrusion," *Polymer Composite* 41(3), 1106-1117. DOI: 10.1002/pc.25442

Bledzki, A., and Faruk, O. (2003). "Wood fibre reinforced polypropylene composites: Effect of fibre geometry and coupling agent on physico-mechanical properties," *Applied Composite Materials* 10, 365-379. DOI: 10.1023/A:1025741100628

Borysiak, S., Paukszta, D., Batkowska, P., and Mankowski, J. (2011). "The structure, morphology, and mechanical properties of thermoplastic composites with ligncellulosic fiber," in: *Cellulose Fibers: Bio- and Nano-Polymer Composites*, S. Kalia, B. S. Kaith, and I. Kaur (eds.), Springer Heidelberg, Dordrecht, Netherlands, pp. 263-290. DOI: 10.1007/978-3-642-17370-7

Burgada, F., Fages, E., Carrillo, L. Q., Lascano, D., Martinez, J. I., Arrieta, M. P., and Fenollar, O. (2021). "Upgrading recycled polypropylene from textile wastes in wood plastic composites with short hemp fiber," *Polymers* 13(8), article 1248. DOI: 10.3390/polym13081248

Cavdar, A. D., Peşman, E., and Torun, S. B. (2023). "Effect of waste toner powder on the performance of microcrystalline cellulose-talc reinforced polypropylene hybrid composites," *Polymer Composites* (Online), article 27832. DOI: 10.1002/pc.27832

Clemons, C. M., and Caufield, D. F. (2005). "Wood flour," in: *Functional Fillers for Plastics*, Wiley-VCH, Weinheim, Germany, pp. 249-270.

Çavdar, A. D., Kalaycıoğlu, H., and Mengeloğlu, F. (2011). "Tea mill waste fibers filled thermoplastic composites: The effects of plastic type and fiber loading," *Journal of Reinforced Plastics and Composites* 30(10), 833-844. DOI: 10.1177/0731684411408752

Çavuş, V. (2020). "Selected properties of mahogany wood flour filled polypropylene composites: The effect of maleic anhydride-grafted polypropylene (MAPP)," *BioResources* 15(2), 2227-2236. DOI: 10.15376/biores.15.2.2227-2236

Çavuş, V., and Mengeloğlu, F. (2020). "Effect of wood particle size on selected properties of neat and recycled wood polypropylene composites," *BioResources* 15(2), 3427-3442. DOI: 10.15376/biores.15.2.3427-3442

Çetin, N. S., Alma, M. H., and Baştürk, M. A. (2000). "Yeni kompozitler üretmek amacıyla doğal lignoselülozik lifler ile sentetik polimerler arasında uyum sağlayan birleştirici maddeler ve metotlar [Chemical agents and methods providing compatibility between ligno-cellulosic fibers and synthetic polymer to obtain new composites]," *Fen ve Mühendislik Dergisi* [*J. Science and Engineering*] 3(2), 58-68.

Díaz, D. H., Ribera, R. V., Julián, F., Tarrés, Q., Espinach, F. X., and Aguilar, M. D. (2020). "Topography of the interfacial shear strength and the mean intrinsic tensile strength of hemp fibers as a reinforcement of polypropylene," *Materials* 13(4), article 1012. DOI: 10.3390/ma13041012

Eroğlu, Ö., Çetin, N. S., Narlıoğlu, N., and Yan, W. (2023). "Plastic/fiber composite using recycled polypropylene and fibers from *Sorghum halepense L.*," *BioResources* 18(2), 3109-3122. DOI: 10.15376/biores.18.2.3109-3122

Espinach, F. X., Julian, F., Verdaguer, N., Torres, L., Pelach, M. A., Vilaseca, F., and Mutje, P. (2013). "Analysis of tensile and flexural modulus in hemp strands/ polypropylene composites," *Composites Part B: Engineering* 47, 339-343. DOI: 10.1016/j.compositesb.2012.11.021

Faruk, O., Bledzki, A. K., Fink, H.-P., and Sain, M. (2012). "Biocomposites reinforced with natural fibers: 2000–2010," *Progress in Polymer Science* 37(11), 1552-1596. DOI: 10.1016/j.progpolymsci.2012.04.003

Gardner, D. J., Han, Y., and Wang, L., (2015). "Wood–plastic composite technology," *Current Forestry Reports* 1(3), 139-150. DOI: 10.1007/s40725-015-0016-6

Gardner, D. J., and Murdock, D. (2010). "Extrusion of wood plastic composites," (https://www.entwoodllc.com/), Accessed 05 June 2023.

Han, H. C., Gong, X. L., Li, C., Kang, F., Yang, H. B., and Zhou, M. (2021). "A study of water-induced elementary hemp fiber swelling and the reinforced polypropylene composite expansion," *Polymer Composites* 42(10), 5101-5110. DOI: 10.1002/pc.26208

Islam, M. R., Mohammad, D. H. B., and Gupta, A. (2013). "Characterization of laccase-treated kenaf fibre reinforced recycled polypropylene composites," *BioResources* 8(3), 3753-3770. DOI: 10.15376/biores.8.3.3753-3770

Kakroodi, A. R., Leduc, S., and Rodrigue, D. (2012). "Effect of hybridization and compatibilization on the mechanical properties of recycled polypropylene-hemp composites," *J. Appl. Polymer Science* 124(3), 2494-2500. DOI: 10.1002/app.35264

Karmarkar, A., Chauhan, S. S., Modak, J. M., and Chanda, M. (2007). "Mechanical properties of wood–fiber reinforced polypropylene composites: Effect of a novel compatibilizer with isocyanate functional group," *Composites Part A: Applied Science and Manufacturing* 38(2), 227-233. DOI: 10.1016/j.compositesa.2006.05.005

Khoathane, M. C., Vorster, O. C., and Sadiku, E. R. (2008). "Hemp fiber-reinforced 1-pentene/polypropylene copolymer: The effect of fiber loading on the mechanical and thermal characteristics of the composites," *Journal of Reinforced Plastics and Composites* 27(4), 1533-1544. DOI: 10.1177/0731684407086325

Klyosov, A. A. (2007). *Wood-plastic Composites*, John Wiley & Sons, Inc., Hoboken, NJ, USA. DOI: 10.1002/9780470165935

Kilic, İ. (2012). *Doğal Lif Katkılı Polistiren Kompozitlerin Üretilmesi ve Mikro Hücre Yöntemiyle Köpüklendirilmesi* [*Natural Fiber Based Polystyrene Composites Manufacturing and Generating of Micro-cell Foams*], Master's Thesis, Kahramanmaraş Sütçü İmam University, Kahramanmaraş, Türkiye.

Kilic, İ., Avcı, B., Atar, İ., Korkmaz, N., Yılmaz, G., and Mengeloğlu, F. (2023). "Using furniture factory waste sawdust in wood plastic composite production and prototype sample production," *BioResources* 18(4), 7212-7229. DOI: 10.15376/biores.18.4.7212-7229

Kim, H.-S., Le, B.-H., Choi, S.-W., Kim, S., and Kim, H.-J. (2007). "The effect of types of maleic anhydride-grafted polypropylene (MAPP) on the interfacial adhesion properties of bio-flour-filled polypropylene composites," *Composites Part A: Applied Sci. Manufacturing* 38(6), 1473-1482. DOI: 10.1016/j.compositesa.2007.01.004

Kim, J. K., and Pal, K. (2010). *Recent Advances in the Processing of Wood–Plastic Composites*, Springer-Verlag Berlin, Germany. DOI: 10.1007/978-3-642-14877-4

Koronis, G., Silva, G., and Fontul, M. (2013). "Green composites: A review of adequate materials for automotive applications," *Composites Part B: Engineering* 44(1), 120-127. DOI: 10.1016/j.compositesb.2012.07.004

Kurek, B. (2013). "Physiology and botany of industrial hemp," in: *Hemp Industrial Production and Uses*, P. Bouloc, S. Allegret, L. Arnaud, D. P. West (eds.), CABI Publishing, Wallingfort, UK, pp. 27-47.

Langhorst, A. E., Burkholder, J., Long, J., Thomas, R., Kiziltas, A., and Mielewski, D. (2018). "Blue-agave fiber-reinforced polypropylene composites for automotive applications," *BioResources* 13(1), 820-835. DOI: 10.15376/biores.13.1.820-835

Li, T. Q., Ng, C. N., and Li, K. Y. (2001). "Impact behavior of sawdust/recycled–PP composites," *Journal of Applied Polymer Science* 81(6), 1420-1428. DOI: 10.1002/app.1567

Lopez, J. P., Vilaseca, F., Barberà, L., Bayer, R. J., Pèlach, M. A., and Mutjé, P. (2012). "Processing and properties of biodegradable composites based on Mater-Bi® and hemp core fibres," *Resources, Conservation and Recycling* 59, 38-42. DOI: 10.1016/j.resconrec.2011.06.006

Lu, J. Z., Wu, Q., and McNabb, H. S. (2000). "Chemical coupling in wood fiber and polymer composites: A review of coupling agents and treatments," *Wood and Fiber Science* 32(1), 88-104.

Manaia, J. P., and Manaia, A. (2021). "Interface modification, water absorption behaviour and mechanical properties of injection moulded short hemp fiber-reinforced thermoplastic composites," *Polymers* 13, article 1638. DOI: 10.3390/polym13101638

Mantia, F. P. L., and Morreale, M. (2011). "Green composites: A brief review," *Composites: Part A* 42, 579-588. DOI: 10.1016/j.compositesa.2011.01.017

Maziero, R., Soares, K., Filho, A. I., Franco, A. R., and Rubio, J. C. C. (2019). "Maleated polypropylene as coupling agent for polypropylene composites reinforced with *Eucalyptus* and *Pinus* particles," *BioResources* 14(2), 4774-4791. DOI: 10.15376/biores.14.2.4774-4791

Mengeloğlu, F., and Karakus, K. (2008). "Some properties of eucalyptus wood flour filled recycled high density polyethylene polymer-composites," *Turkish Journal of Agriculture & Forestry* 32(6), 537-546.

Mengeloglu, F., and Karakuş, K. (2012). "Mechanical properties of injection-molded foamed wheat straw filled HDPE biocomposites: The effects of filler loading and coupling agent contents," *BioResources* 7(3), 3293-3305. DOI: 10.15376/biores.7.3.3293-3305

Mengeloğlu, F., Başboğa, H. İ., and Aslan, T. (2015). "Selected properties of furniture plant wasted filled thermoplastic composites," *PROLIGNO* 11(4), 199-206.

Mengeloğlu, F. (2020). *Kenevirin Kompozit Sanayisinde ve Kağıt Üretiminde Kullanımı: Kenevir (Cannabis sativa L.), [Use of Hemp in Composite Industry and Paper Production: in: Hemp (Cannabis sativa L.)]*, A. Onay, H. Yıldırım, and R. Ekinci (eds.), Palme Yayınevi, Ankara, Türkiye.

Mengeloğlu, F., and Çavuş, V. (2020). "Preparation of thermoplastic polyurethane-based biocomposites through injection molding: Effect of the filler type and content," *BioResources* 15(3), 5749-5763. DOI: 10.15376/biores.15.2.2227-2236

Mohanty, A. K., Misra, M., and Drzal, L. T. (2001). "Surface modifications of natural fibers and performance of the resulting biocomposites: An overview," *Composite Interfaces* 8(5), 313-343. DOI: 10.1163/156855401753255422

Mohanty, A. K., Misra, M., and Drzal, L. T., (2002). "Sustainable bio-composites from renewable resources: Opportunities and challenges in the green materials world," *Journal of Polymers and the Environment* 10, 19-26

Montanes, N., Carrillo, L. Q., Ferrandiz, S., Fenollar, O., and Boronat, T. (2019). "Effects of lignocellulosic fillers from waste thyme on melt flow behavior and processability of wood plastic composites (WPC) with biobased poly(ethylene) by injection molding," *Journal of Polymers and the Environment* 27, 747-756. DOI: 10.1007/s10924-019-01388-0

Narlıoğlu, N., Çetin, N. S., and Alma, M. H. (2018). "Karaçam testere talaşının polipropilen kompozitlerin mekanik özelliklerine etkisi [Effect of black pine sawdust on the mechanical properties of polypropylene composites]," *Mobilya ve Ahşap Malzeme Araştırmaları Dergisi [Furniture and Wooden Material Research Journal]* 1(1), 38-45. DOI: 10.33725/mamad.433532

Oksman, K., Mathew, A. P., Långström, R., Nyström, B., and Joseph, K. (2009). "The influence of fibre microstructure on fibre breakage and mechanical properties of natural fibre reinforced polypropylene," *Composites Science and Technology* 69(11-12), 1847-1853. DOI: 10.1016/j.compscitech.2009.03.020

Panaitescu, D. M. P., Vuluga, Z., Sanporean, C. G., Nicolae, C. A., Gabor, A. R., and Trusca, R. (2019). "High flow polypropylene/SEBS composites reinforced with differently treated hemp fibers for injection molded parts," *Composites Part B: Engineering* 174, article ID 107062. DOI: 10.1016/j.compositesb.2019.107062

Panthapulakkal, S., and Sain, M. (2007). "Injection-molded short hemp fiber/glass fiber reinforced polypropylene hybrid composites-mechanical, water absorption and thermal properties," *Journal of Applied Polymer Science* 103(4), 2432-2441. DOI: 10.1002/app.25486

Pickering, K. L., Efendy, M. G. A., and Le, T. M. (2016). "A review of recent developments in natural fibre composites and their mechanical performance," *Composites Part A: Applied Science and Manufacturing* 83, 98-112. DOI: 10.1016/j.compositesa.2015.08.038

Rey, R. D., Serrat, R., Alba, J., Perez, I., Mutje, P., and Espinach, F. X. (2017). "Effect of sodium hydroxide treatments on the tensile strength and the interphase quality of hemp core fiber-reinforced polypropylene composites," *Polymers* 9(08), article 377. DOI: 10.3390/polym9080377

Rouway, M., Nachtane, M., Tarfaoui, M., Chakhchaoui, N., Omari, L. H., Fraija, F., and Cherkaoui, O. (2020). "Prediction of mechanical performance of natural fibers polypropylene composites: A comparison study," *IOP Conference Series: Materials Science and Engineering* 948, article ID 012031. DOI: 10.1088/1757-899X/948/1/012031

Shahzad, A. (2011). "Hemp fiber and its composites," *Journal of Composite Materials* 46(8) 973-986. DOI: 10.1177/0021998311413623

Silveira, P. H. P. M., Santos, M. C. C., Chaves, Y. S., Ribeiro, M. P., Marchi, B. Z., Monteiro, S. N., Gomes, A. V., Tapanes, N. L. C, Pereira, P. S. C., and Bastos, D. C. (2023). "Characterization of thermo-mechanical and chemical properties of polypropylene/hemp fiber biocomposites: Impact of maleic anhydride compatibilizer and fiber content," *Polymers* 15(15), article 3271. DOI: 10.3390/polym15153271

Stokke, D. D., and Gardner D. J. (2003). "Fundamental aspects of wood as a component of thermoplastic composites," *Journal of Vinyl & Additive Technology* 9(2), Article Number 10069. DOI: 10.1002/vnl.10069

Sullins, T., Pillay, S., Komus, A., and Ning, H. (2017). "Hemp fiber reinforced polypropylene composites: The effects of material treatments," *Composites Part B: Engineering* 114, 15-22. DOI: 10.1016/j.compositesb.2017.02.001

Summerscales, J., Dissanayake, P. J., Virk, A. S., and Hall, W. (2010). "A review of bast fibres and their composites. Part 1- Fibres as reinforcements," *Composites Part A: Applied Science and Manufacturing* 41(10), 1329-1335. DOI: 10.1016/j.compositesa.2010.06.001

Şeker Hirçin, B., Yörür, H., and Mengeloğlu, F. (2021). "Effects of filler type and content on the mechanical, morphological, and thermal properties of waste casting polyamide 6 (W-PA6G)-based wood plastic composites," *BioResources* 16(1), 655-668. DOI: 10.15376/biores.16.1.655-668

Vallejos, M. E., Vilaseca, F., Méndez, J. A., Espinach, F. X., Aguado, R. J., Aguilar, M. D., and Mutjé, P. (2023). "Response of polypropylene composites reinforced with natural fibers: Impact strength and water-uptake behaviors," *Polymers* 15(4), article 900. DOI: 10.3390/polym15040900

Vilasecaa, F., Reyb, R. D., Serratc, R., Albab, J., Mutjec, P., and Espinach, F. X. (2018). "Macro and micro-mechanics behavior of stiffness in alkaline treated hemp core fibres polypropylene-based composites," *Composites Part B: Engineering* 144, 118-125. DOI: 10.1016/j.compositesb.2018.02.029

Vilaseca, F., Parareda, S. P., Espinosa, E., Rodríguez, A., Mutjé, P., and Aguilar, M. D. (2020). "Valorization of hemp core residues: Impact of NaOH treatment on the flexural strength of PP composites and intrinsic flexural strength of hemp core fibers," *Biomolecules* 10(6), article 823. DOI: 10.3390/biom10060823

Wu, H., Xu, D., Zhou, Y., Gao, C., Guo, J., He, W., He, Y., and Qin, S. (2020). "Tung oil anhydride modified hemp fiber/polypropylene composites: The improved toughness, thermal stability and rheological property," *Fibers and Polymers* 21(9), 2084-2091. DOI: 10.1007/s12221-020-1157-1

Wu, H., Xu, D., Zhou, Y., Guo, J., He, W., He, Y., Yi, Y., and Qin, S. (2021). "The improved mechanical and thermal properties of hemp lifs reinforced polypropylene composites with dodecyl bromide modification," *Fibers and Polymers* 22(6), 2869-2877. DOI: 10.1007/s12221-021-0127-6

Yan, Z., Zhang, J., Zhang, H., and Wang, H. (2013). "Improvement of mechanical properties of noil hemp fiber reinforced polypropylene composites by resin modification and fiber treatment," *Advances in Materials Science and Engineering* 2013, article ID 941617. DOI: 10.1155/2013/941617

Yang, H. S., Kim, H. J., Son, J., Park, H. J., Lee, B. J., and Hwang, T. S. (2004). "Rice-husk flour filled polypropylene composites; mechanical and morphological study," *Composite Structures* 63(3-4), 305-312. DOI: 10.1016/S0263-8223(03)00179-X

Yang, H. S., Kim, H. J., Park, H. J., Lee, B. J., and Hwang, T. S. (2007). "Effect of compatibilizing agents on rice-husk flour reinforced polypropylene composites," *Composite Structures* 77(1), 45-55. DOI: 10.1016/j.compstruct.2005.06.005

Yuan, Q., Wu, D., Gotama, J., and Bateman, S. (2008). "Wood fiber reinforced polyethylene and polypropylene composites with high modulus and impact strength," *Journal of Thermoplastic Composite Materials* 21(3), 195-208. DOI: 10.1177/0892705708089472

Zaini, M. J., Fuad, M. Y. A., Ismail, Z., Mansor, M. S., and Mustafah, J. (1996). "The effect of filler content and size on the mechanical properties of polypropylene/oil palm wood flour composites," *Polymer International* 40(1), 51-55. DOI: 10.1002/(SICI)1097-0126(199605)

Article submitted: December 5, 2023; Peer review completed: January 3, 2024; Revised version received: January 4, 2024; Accepted: January 11, 2024; Published: January 16, 2024.
DOI: 10.15376/biores.19.1.1494-1516